Beilstein-Institut
Experimental Standard Conditions of Enzyme Characterization
September 12th – 16th, 2011, Rüdesheim/Rhein, Germany

Protein Engineering Elucidates the Relationship between Structure, Function and Stability of a Metabolic Enzyme

Reinhard Sterner, Thomas Schwab and Sandra Schlee

University of Regensburg, Institute of Biophysics and Physical Biochemistry, Universitätsstrasse 31, D-93053 Regensburg, Germany.

E-Mail: *Reinhard.Sterner@biologie.uni-regensburg.de

Received: 14th March 2012/Published: 15th February 2013

Abstract

The relationship between oligomerisation state, stability, and catalytic activity of the anthranilate phosphoribosyl transferase from *Sulfolobus solfataricus* (sAnPRT) was analysed by three interrelated protein engineering approaches. The extremely thermostable homodimeric sAnPRT enzyme was converted into a monomer by rational design, and its low catalytic activity at 37 °C was elevated by a combination of random mutagenesis and metabolic selection in the mesophilic host *Escherichia coli*. The two amino acid exchanges leading to monomerization and the two substitutions resulting in activation of sAnPRT were then combined, which resulted in an "activated monomer" that was significantly less stable and more active than wild-type sAnPRT. Using a combination of random mutagenesis and selection in the thermophilic host *Thermus thermophilus*, the activated monomer was stabilized, and the consequences of stabilization for catalytic activity and association state were analysed.

Introduction

It is important to understand how the tertiary and quaternary structure of an enzyme determines its thermal stability, catalytic activity, and conformational flexibility. Insights into the interrelationship between these properties were gained by the analysis of homologous enzymes from mesophiles and hyperthermophiles that are characterized by an optimum growth temperature close to the boiling point of water [1]. For example, crystal structure analysis suggests that the significantly higher stability of enzymes from hyperthermophiles compared to their counterparts from mesophiles is due to only minor modifications at the level of tertiary structure: a slightly elevated number of hydrogen bonds or salt bridges, a higher compactness, an increased polar to non-polar surface area, and raises in α-helix content and α-helix stability. At the level of quaternary structure, more pronounced differences have been observed occasionally: some enzymes from hyperthermophiles form higher-order oligomers than the homologous proteins from mesophiles [2, 3].

In natural enzymes, conformational integrity at high temperatures generally comes along with low catalytic activity at room temperature. This negative stability – activity correlation is understandable from a *biological* point of view: enzymes from hyperthermophiles do not need to catalyse reactions at 25 °C, and enzymes from mesophiles do not have to resist 100 °C in their natural habitats. From a *physicochemical* point of view, the pronounced differences in activity between mesophilic – thermophilic enzyme pairs when compared at identical temperatures must be due to subtle alterations in the protein chain, because the active site residues are conserved among homologous enzymes, independent of the growth optimum of the host organism [4]. Having in mind that enzymatic activity requires a certain degree of flexibility [5], it has been speculated that the low activity of thermostable enzymes at mesophilic temperatures is due to high conformational rigidity, which is relieved at elevated temperature. As a consequence, mesophilic – thermophilic enzyme pairs should be comparably flexible and active at the respective physiological conditions [6]. However, the general validity of this concept of 'corresponding states' [7] has remained under debate [8, 9].

Although interesting and attractive, the explanatory power of comparisons between homologous enzymes from mesophiles and hyperthermophiles is severely limited by the high degree of sequence diversity, which has accumulated in during the course of natural evolution. Even for a comparably high sequence conservation of 50% between a hypothetical pair of enzymes containing 200 residues, 100 amino acids are disparate. However, typically no more than about five residue substitutions will be responsible for differences in stability or catalysis, which can make their identification a laborious and time-consuming 'needle in the haystack' search.

An alternative approach for identifying minor structural modifications that cause substantial alterations of enzyme integrity and function is protein engineering, which can be performed either by rational design or directed laboratory evolution. Rational protein design approaches are generally based on high-resolution crystal structures that guide the introduction of amino acid exchanges at specific positions with preconceived effects on protein stability or activity [10]. The protein variants are produced by site-directed mutagenesis and purified, and the effects of the substitutions are analysed, typically by enzyme kinetics, unfolding studies, and structural analysis. In a directed evolution experiment amino acid exchanges are not introduced at predetermined positions but are incorporated at random sites, typically by error-prone PCR. From the resulting gene library, variants with elevated stability or activity are isolated by *in vivo* selection or high-throughput *in vitro* screening. Directed evolution often leads to surprising solutions with beneficial amino acid exchanges at unexpected positions, which makes this approach particularly instructive [11]. Importantly, variants generated by rational design or directed evolution typically carry only a few amino acid substitutions, a feature that considerably alleviates their analysis. Rational design and directed evolution experiments have shown that the increase of catalytic power comes at the expense of a reduced conformational stability, and *vice versa*. However, in a few cases, both enzymatic properties could be optimized simultaneously, supporting the notion that the trade-off between catalysis/flexibility and stability observed in natural proteins is not due to physicochemical constraints [12].

In the following, the results of protein engineering studies will be presented that were performed to elucidate the structure-function-stability relationship of anthranilate phosphoribosyl transferase from *Sulfolobus solfataricus* (sAnPRT), which is a hyperthermophilic archaeon with an optimum growth temperature of 80 °C. Phosphoribosyl transferases (PRTases) are involved in the metabolism of nucleotides and amino acids. They catalyse the Mg^{2+}-dependent displacement of pyrophosphate (PP_i) from 5'-phosphoribosyl-α1-pyrophosphate (PRPP) by a nitrogen-containing nucleophile, producing an α-substituted ribose-5-phosphate. On the basis of their tertiary structures, PRTases have been divided into three different classes. Members of class I are the orotate and uracil PRTases as well as the purine PRTases. Representatives of class II are the quinolinate and nicotinic acid PRTases [13]. The only known member of class III is anthranilate phosphoribosyltransferase (AnPRT), which is encoded by the *trp*D gene and catalyses the third step of tryptophan biosynthesis, the ribosylation of anthranilate to phosphoribosyl anthranilate (PRA) (Figure 1).

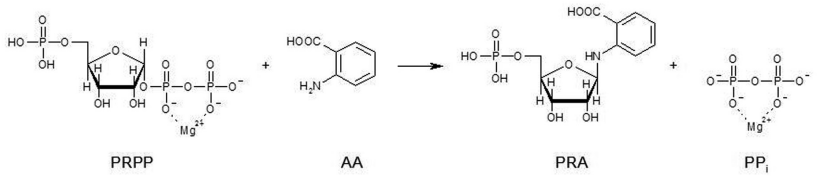

Figure 1. Reaction catalysed by AnPRT. PRPP, 5'-phophoribosyl-α1-pyrophosphate; AA, anthranilate; PRA, *N*-(5'-phosphoribosyl)anthranilate; PP_i, pyrophosphate.

Results

Monomerisation of homodimeric sAnPRT by rational protein design

Figure 2A shows a ribbon diagram of the structure of sAnPRT, which was solved in complex with two molecules of anthranilate (AA) and one molecule of PRPP [14].

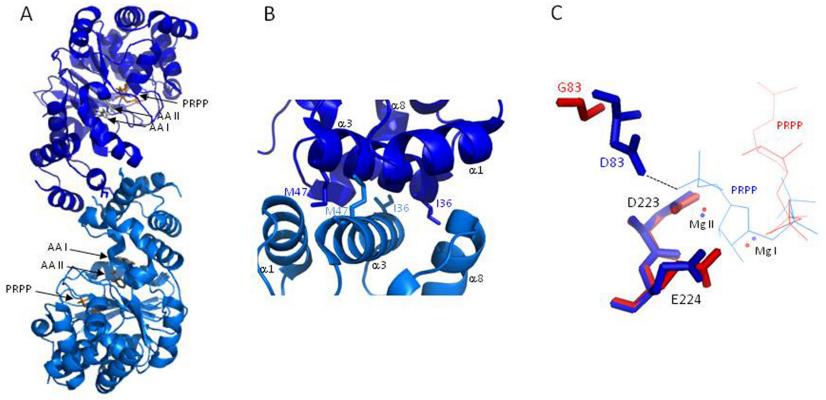

Figure 2. Crystal structures of sAnPRT. **(A)** Ribbon diagram of dimeric sAnPRT with bound substrates anthranilate (AA I and AA II) and PRPP. **(B)** Dimer interface of sAnPRT formed by helices α1, α3, and α8. Residues I36 and M47, which are located at the N- and C-termini of helix α3, are displayed as sticks. **(C)** Plot of PRPP and metal coordination by wild-type sAnPRT (blue) and sAnPRT-D 83G+F149S (red). The structures have been superimposed on the main chain atoms of the conserved acidic motif (D 223-E224). The hydrogen bond between the 5'-phosphate group of PRPP with the carboxyl side chain of aspartate 83 is indicated by a dashed line.

The enzyme forms a homodimer of identical subunits that consist of two domains: a large α/β domain, formed by a central β-sheet together with a C-terminal cluster of eight helices, and a small α-helical domain, comprising six helices. The substrate binding cavity for the coordination of two molecules of AA, one molecule of PRPP, and two Mg^{2+}-ions (Mg-I and Mg-II) is located at the domain interface, while dimer formation is mediated by the small

α-helical domains which associate in a head-to-head fashion displaying an approximate two-fold symmetry. Wild-type sAnPRT is extremely thermostable with a half-life at 85 °C of 35 min [15] and catalytically proficient at 60 °C with a turnover number of 4.2 s^{-1} [14], but only marginally active at 37 °C with a turnover number of 0.33 s^{-1}.

In order to elucidate the significance of homo-dimer formation for stability and activity of sAnPRT, the enzyme was monomerised by performing rational design on the basis of the crystal structure of the enzyme. Residues crucial for dimer formation were identified by inspecting the interface of the two protomers, which is mainly formed by residues from helices α1, α3 and α8 (Figure 2B). An *in silico* analysis suggested that the hydrophobic residues Ile36 and Met47, which are located at the N- and C-termini of helix α3, form the most numerous and intimate reciprocal inter-subunit interactions. Based on this finding, site-directed mutagenesis was used to replace Ile36 and Met47 by the acidic residues glutamate and aspartate, both individually and in combination. We reasoned that the introduction of the negatively charged side chains would weaken the stabilizing interactions of Ile36 and Met47 with residues of the other subunit. Moreover, the relatively low distances between the C_β-atoms of the symmetry-related Ile36-Ile36' (6.8 Å) and Met47-Met47' (4.4 Å) residue pairs indicated that the introduced negative charges further weaken inter-subunit interactions by electrostatic repulsion. Moreover, negatively charged residues located at the surface increase protein solubility, which could stabilize the monomer. Met47 was replaced by aspartate instead of glutamate, because its shorter side chain has a lower probability of forming a stabilizing hydrogen bond with Lys13' from the neighbouring protomer.

The double variant sAnPRT-I36E+M47D and the two single variants sAnPRT-I36E and sAnPRT-M47D were produced in *E. coli* and purified, and their association state was assessed by gel filtration chromatography and analytical ultracentrifugation. The results demonstrated that the double variant formed a homogeneous monomer, whereas the single variants were present in adimer-monomer equilibrium. Steady-state enzyme kinetics performed at 37 °C showed that sAnPRT-I36E+M47D has, within experimental error, an identical turnover number (k_{cat}) as the wild-type enzyme and unaltered Michaelis constants for AA (K_m^{AA}) and PRPP (K_m^{PRPP}). In contrast, differential scanning calorimetry and thermal inactivation revealed that the melting temperature (T_M) of sAnPRT-D 83G+F149S was decreased by ~ 10 °C and that its inactivation at 80 °C ($t_{1/2(80\ °C)}$) was accelerated ~ 10-fold. In order to discriminate between destabilization caused by the substitutions *per se* from destabilization caused by monomerisation, inactivation kinetics were performed in presence of various protein concentrations. At the lowest applied subunit concentration, sAnPRT-I36E and sAnPRT-M47D were present as monomers, and their $t_{1/2(80°C)}$ values of 4 min and 3 min were identical to the concentration-independent half-life of sAnPRT-I36E+M47D. At the highest tested concentrations, sAnPRT-I36E and sAnPRT-M47D became completely or partly dimeric, and their $t_{1/2(80°C)}$ values of about 40 min and 15 min approached the concentration-independent half-life of wild-type sAnPRT.

These results prove that the introduced amino acid substitutions did not influence inactivation kinetics significantly, and that the higher stability of wild-type sAnPRT compared to sAnPRT-I36E+M47D is mainly due to dimerisation. We concluded that the monomeric double variant of sAnPRT resembles the experimentally inaccessible isolated wild-type subunits, and that sAnPRT is a dimer for reason of stability but not activity [16].

Activation of sAnPRT by library selection in Escherichia coli

The goal of this study was to increase the low catalytic activity of sAnPRT at 37 °C, and to assess the consequences of activation for thermal stability. Although the crystal structure with bound anthranilate, PRPP, and Mg^{2+}allowed for the identification of individual residues involved in substrate binding, it provided no hint as to which amino acid exchanges might lead to the activation of the enzyme. Given the absence of a rationale for pre-assigned substitutions, we turned to a combination of random mutagenesis and selection *in vivo*. For this purpose, the s*trp*D gene encoding sAnPRT was amplified by error-prone PCR under conditions that led to the introduction of an average of 2 – 3 amino acid exchanges of the protein. The amplification products were ligated into a plasmid that allows for gene expression in *E. coli*. The ligation mixture was used to transform an *E. coli* Δ*trp*EGD strain lacking the first three genes of the tryptophan biosynthetic pathway, which encode the anthranilate synthase complex (*trp*E and *trp*G code for the large and small subunit, respectively) and AnPRT (*trp*D). For growth on medium plates without tryptophan, Δ*trp*EGD requires externally added anthranilate and transformation with a *trp*D gene that codes for an AnPRT with significant catalytic activity at 37 °C. Whereas Δ*trp*EGD cells transformed with wild-type s*trp*D needed 80 h to form colonies on minimal medium supplemented with anthranilate, a number of cells transformed with the plasmid mixture containing randomized s*trp*D grew to a visible size within 16 – 48 h. The faster growing colonies were expected to produce sAnPRT variants with a higher catalytic activity than the wild-type enzyme at 37 °C, which is more than 40 degrees below the physiological temperature of *S. solfataricus*. Sequencing of the s*trp*D inserts isolated from the fastest growing colonies revealed mutations that resulted in the exchange of aspartate 83 by glycine (D 83G) or asparagine (D 83N), and the substitution of phenylalanine 149 by serine (F149S).

The double variants AnPRT-D 83G+F149S and the two single variants sAnPRT-D 83G and sAnPRT-F149S were produced in *E. coli* and purified. Analytical gel filtration chromatography showed that all three variants retained the homodimeric association state of wild-type sAnPRT. Steady-state enzyme kinetics performed at 37 °C demonstrated that the pronounced inhibition of wild-type sAnPRT by high concentrations of Mg^{2+} was no longer present in sAnPRT-D 83G+F149S and sAnPRT-D 83G. In order to explain this observation, sAnPRT-D 83G+F149S was crystallized in presence of PRPP and Mn^{2+}, which can be identified more reliably in electron density maps than Mg^{2+}. The analysis of the X-ray structure revealed that PRPP bound to sAnPRT-D 83G+F149S adopts an extended conformation that contrasts markedly with the "S" compact shape observed in complexes of wild-type sAnPRT

(Figure 2C). The ‘‘S’’ shape of PRPP in the wild-type enzyme is stabilized by a hydrogen bond between the 5’-phosphate group of the substrate with the carboxyl side chain of aspartate 83. Within sAnPRT-D 83G+F149S, the hydrogen bond is lost as a result of the D 83G exchange. For wild-type sAnPRT, the 5’-phosphate group of PRPP is involved in the binding of the second Mg^{2+}-ion (Mg-II). Although a second bivalent cation is also present in sAnPRT-D 83G+F149S, the 5’-phosphate group of the extended PRPP is too far away to contribute to its binding. We therefore speculated that the affinity of Mg-II for the active site might be decreased in sAnPRT-D 83G+F149S and thus the propensity for the transformation of the productive PRPP*Mg-I complex into a putatively inhibitory Mg-II*PRPP*Mg-I complex might be lower in the double variant than in wild-type sAnPRT. This assumption was confirmed by the thorough analysis of the PRPP- and Mg^{2+}-dependent enzymatic activities of wild-type sAnPRT and sAnPRT-D 83G+F149S [17].

In addition to abolishing inhibition by Mg^{2+}, the two amino acid substitutions activate wild-type sAnPRT by a 40-fold enhancement of the turnover number at 37 °C in presence of the respective optimum concentrations of Mg^{2+} (wild-type sAnPRT: $k_{cat} = 0.33\ s^{-1}$, 37 °C, 50 µM Mg^{2+}; sAnPRT-D 83G+F149S: $k_{cat} = 13.3\ s^{-1}$, 37 °C, 2 mM Mg^{2+}). Pre-steady state kinetic measurements were performed to determine the rate-limiting step of the AnPRT reaction, which – according to the differences in k_{cat} – is accelerated 40-fold for sAnPRT-D 83G+F149S compared to wild-type sAnPRT. The minimal kinetic reaction scheme used to analyse the data is shown in Figure 3.

Figure 3. Minimal catalytic mechanism of the sAnPRT reaction with first-order rate constants describing the chemical transfer step (k_{trans}) and product release (k_{off}).

After the formation of the sAnPRT*AA*PRPP complex, a phosphoribosyl moiety is transferred from PRPP to AA (described by k_{trans}), followed by the release of the products PRA and PP_i (described by k_{off}). The turnover number measured in the steady-state is determined by the chemical transfer and product release steps as follows: $k_{cat} = (k_{trans} \times k_{off})/(k_{trans} + k_{off})$. Therefore, the increase in k_{cat} observed for sAnPRT-D 83G+F149S could be caused by an increase of either k_{trans} or k_{off}, depending on whether product release is comparably fast and chemical transfer is rate-limiting ($k_{trans}<k_{off}$), or *vice versa* ($k_{trans}>k_{off}$). To distinguish between the two possibilities, the turnover numbers of wild-type sAnPRT and sAnPRT-D 83G+F149S determined by steady-state kinetics were compared with the value of k_{trans} as determined from transient kinetic experiments performed under single turnover conditions in a stopped-flow apparatus. For this purpose, a pre-incubated solution containing AA and an excess of sAnPRT was rapidly mixed with saturating concentrations of PRPP in presence of the respective optimal concentration of Mg^{2+}. Under conditions where the formation of sAnPRT*AA*PRPP is complete within the dead-time of the experiment (sAnPR-

T*AA*PRPP ≈ $[A]_{total}$; single-turnover conditions), the reaction is described by a two-step irreversible process (Figure 3). Since the spectroscopic change occurs upon product formation at the active site of the enzyme, the observed first-order rate constant k_{obs} corresponds to k_{trans}. An analysis of the dependence of k_{obs} on enzyme concentration yielded $k_{trans} = 29.6 \pm 0.9\ s^{-1}$ for sAnPRT-D83G+F149S, and $k_{trans} > 3.3 \pm 0.16\ s^{-1}$ for sAnPRT. From the relationship $k_{cat} = (k_{trans} \times k_{off})/(k_{trans} + k_{off})$, it follows that $k_{off} = 24.2 \pm 2.0\ s^{-1}$ for the double variant and $k_{off} \sim 0.33\ s^{-1}$ for the wild-type enzyme. For sAnPRT-D83G+F149S $k_{trans} \sim k_{off}$, demonstrating that phosphoribosyl transfer and product release affect catalytic turnover equally. For wild-type sAnPRT $k_{trans} > k_{off} = k_{cat}$, showing that product release determines the overall catalytic rate. In summary, the comparison of steady-state and single turnover data shows that the increased turnover number of sAnPRT-D83G+F149S is mainly based on the accelerated liberation of product. Since dissociation of PP_i has been shown to be fast in other PRTases [18], the two amino acid exchanges appear to facilitate the release of PRA from the enzyme.

Differential scanning calorimetry and thermal inactivation revealed that the melting temperature of sAnPRT-D83G+F149S was decreased by ~10 °C and its inactivation at 80 °C was accelerated ~10-fold. The analysis of the two single variants showed that this destabilization is entirely caused by the F149S exchange. Remarkably, F149 is located within the hinge between the two domains of the sAnPRT protomer. One can speculate that a substitution at this position has an influence on the dynamics of *bona fide* domain opening and closure movements, which might be required for the release of PRA. Along these lines, it has been shown for glutathione transferase that an increase in local flexibility can accelerate the rate-limiting release of product in the millisecond time range (for sAnPRT-D83G+F149S: $k_{off} = 25\ s^{-1}$, $t_{1/2} = 28$ ms), a time scale that is similar to that expected for the upper limit of large amplitude segmental motions [19]. For sAnPRT-wt, the k_{cat} value increases from $0.33\ s^{-1}$ at 37 °C to $4.2\ s^{-1}$ at 60 °C [14], suggesting that the velocity of product release, which limits the activity of the parental protein at 37 °C, is accelerated at 60 °C by a similar increase in flexibility as by the F149S replacement at 37 °C [17].

Stabilisation of the activated sAnPRT monomer by library selection in **Thermus thermophilus**

We were interested to assess the effect of combining the amino acid exchanges leading to monomerisation (I36E, M47D) and activation (D83G, F149S) of sAnPRT. For this purpose, the *strp*D-I36E+M47D+D83G+F149S gene was generated by site-directed mutagenesis and expressed in *E. coli*. The recombinant sAnPRT-I36E+M47D+D83G+F149S protein (''activated monomer'') was purified and characterized. Steady-state enzyme kinetics and thermal unfolding using DSC and far-UV CD spectroscopy yielded a k_{cat} at 37 °C of $3.4\ s^{-1}$ and a T_M of ~70 °C. Consequently, the turnover number is 10-fold higher and the melting temperature 20 °C lower compared to wild-type sAnPRT. The results show that the activating effect of

the D 83G and F149S exchanges is somewhat less pronounced in the monomer than in the dimer, and that the destabilizing effects caused by monomerization and activation (both modifications lead to a decrease of T_M by ~10 °C) sum up in the activated monomer.

We attempted to "re-stabilize" sAnPRT-I36E+M47D+D 83G+F149S by a combination of random mutagenesis and metabolic selection in *Thermus thermophilus*. This extremely thermophilic bacterium is an ideal host for protein stabilization by library selection, because it grows between 55 °C and 80 °C and has a high natural competence for DNA uptake. Due to these properties, *T. thermophilus* cells transformed with a gene library can be incubated at elevated temperatures where survival of the host depends on the stabilization of the target protein. Taking advantage of the high transformation efficiency of *E. coli*, we used the mesophilic host for the generation of a large plasmid-encoded library of the *strp*D-I36E+M47D+D 83G+F149S gene. For this purpose, the gene was amplified by error-prone PCR, and the resulting repertoire was ligated into an *E. coli-T. thermophilus* shuttle plasmid. Transformation of highly competent *E. coli* cells yielded a library consisting of 9×10^6 individual plasmid-encoded mutants carrying a various number of nucleotide exchanges.

The shuttle plasmids were isolated and used to transform a *T. thermophilus* Δ*trp*D strain, which requires for growth in the absence of tryptophan a *trp*D gene encoding an AnPRT with high thermal stability. Control experiments showed that Δ*trp*D cells transformed with *strp*D-I36E+M47D+D 83G+F149S allowed for growth on selective medium up to only 70 °C, whereas transformation with wild-type *strp*D yielded colonies up to 79 °C. A number of Δ*trp*D cells transformed with the plasmid library were also able to grow at 79 °C, indicating that they contained variants with a higher thermal stability than sAnPRT-I36E+M47D+D 83G+F149S. Sequencing of the s*trp*D inserts isolated from 20 colonies revealed that the selected variants contained three amino acid exchanges on average. For further analysis, we focused on the T77I, N109S, I169T, F193S and L 320 M substitutions, which either occurred as single exchange in a selected variant or were found independently in at least two different variants. The exchanges were introduced individually into the *strp*D-I36E+M47D+D 83G+F149S gene by site-directed mutagenesis, and the recombinant proteins were produced in *E. coli*, purified, and characterized. Thermal unfolding revealed that the T77I and F193S substitutions resulted in considerable T_M-increases of approximately 8 °C and 4 °C, whereas each of the N109S, I169T and L 320 M exchanges lead to a stabilization by only about 1 °C. The combination of the beneficial mutations showed that the T_M increases were additive to a first approximation. As a consequence, the variant containing all five identified stabilizing exchanges displayed a T_M of about 83.5 °C, which is 13 °C higher than the melting temperature of sAnPRT-I36E+M47D+D 83G+F149S (Figure 4).

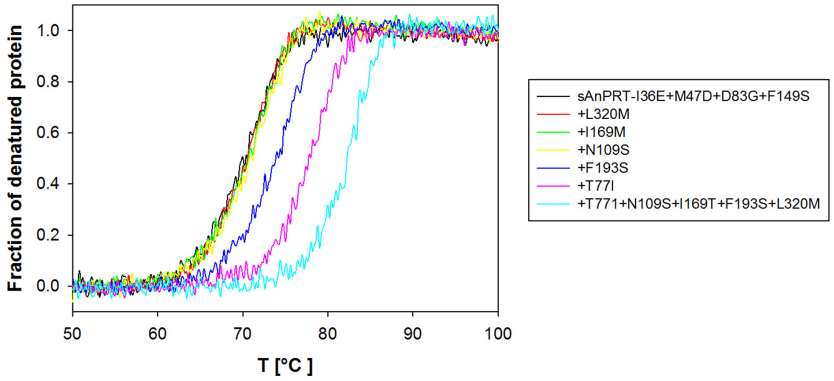

Figure 4. Stabilizing effect of amino acid exchanges identified by library selection in *T. thermophilus*. Thermal unfolding traces were recorded by loss of the far-UV CD signal at 220 nm.The staring construct sAnPRT-I36E+M47D+D 83G+F149S has aT_M-value of 70.5 °C, which is increased to 83.5 °C by the combined substitutions T77I+N109S+I169T+F193S+L 320 M.

The T77I, N109S, I169T, F193S and L 320 M substitutions are distributed all over the structure of sAnPRT. Computational modelling suggests that replacing the polar side chain of threonine with the larger hydrophobic side chain of isoleucine (T77I) fills a cavity in the protein interior, explaining the strong increase of thermal stability caused by this exchange. In the absence of a high resolution crystal structure, the basis for the stabilizing effect of the other, less beneficial substitutions has remained unclear so far. In any case, analytical gel filtration showed that all variants were monomeric, demonstrating that stabilization was not due to "re-dimerization" of sAnPRT.

The catalytic activity of sAnPRT-I36E+M47D+D 83G+F149S and its stabilized variants was measured by steady-state enzyme kinetics at 37 °C. As outlined in the previous section, the D 83G exchange leads to the removal of the inhibition of wild-type sAnPRT by high concentrations of Mg^{2+}. Accordingly, sAnPRT-I36E+M47D+D 83G+F149S and its variants are maximally active in the presence of millimolar concentrations of the bivalent cation. The two strongly stabilizing exchanges T77I and F193S modestly reduce the k_{cat} of sAnPRT-I36E+M47D+D 83G+F149S by a factor of 2.5 and 1.3, respectively. Activity is stronger affected by the N109S exchange, which results in a 4.5-fold reduction of k_{cat}, probably because it is located close to the active site. The two stabilizing mutations I169T and L 320 M do not significantly alter the turnover number.

In order to obtain a comprehensive picture about the stability-activity relationship, the k_{cat}-values at 37 °C of all characterized monomeric sAnPRT variants were plotted as a function of the respective T_M (Figure 5).

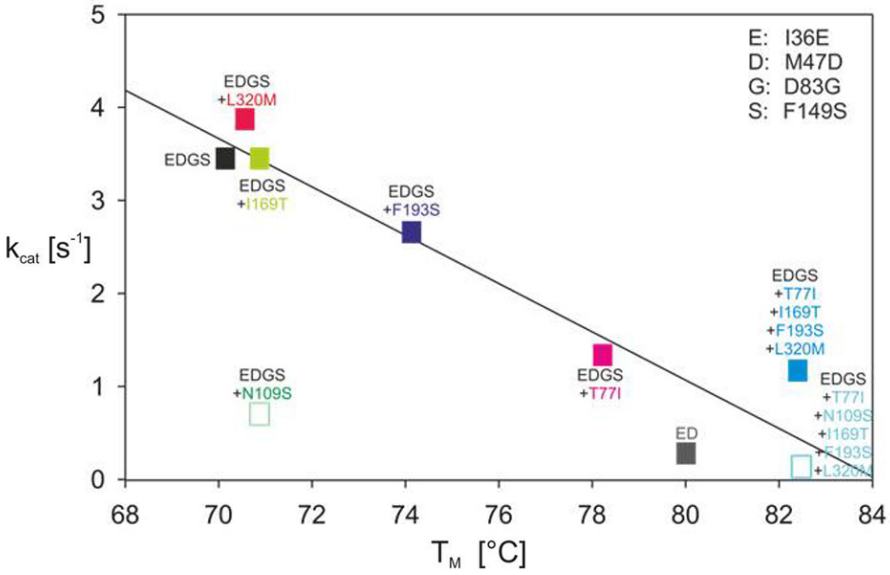

Figure 5. Negative correlation between turnover number and thermal stability of monomeric sAnPRT variants. The k_{cat} values at 37 °C were plotted as function of T_M. A negative linear correlation ($r^2 = 0.88$) is observed. Variants carrying the N109S substitution were excluded from the analysis, because this exchange is located close to the active site.

The observed negative correlation is in line with the view that protein flexibility is important for sAnPRT catalysis [20].

Conclusions

The three projects presented in this contribution underline the relevance of protein engineering for elucidating the relationship between the quaternary structure, the catalytic activity and the thermodynamic stability of metabolic enzymes. The non-covalent association of polypeptide chains can have various consequences for enzyme function, for example it can allow for the formation of complex sites or enable substrate channelling [21, 22]. However, the monomerization of sAnPRT [16] and a similar study performed with the homodimeric phosphoribosyl anthranilate isomerase from the hyperthermophile *Thermotoga maritima* [23] show that these enzymes are dimers for stability but not for activity reasons. Whereas the monomerization of sAnPRT was based on the analysis of the crystal structure of the protein, our limited understanding of enzyme-catalysed phosphoribosyl transfer did not allow for a rationale approach to increase the weak activity of sAnPRT at low temperatures. We therefore used directed evolution including random mutagenesis and selection in a mesophilic host to achieve this goal. This approach led to the identification of two *a priori* unpredictable activating amino acid exchanges whose effects on catalysis and stability were

comprehensively analysed. An analogous directed evolution approach, which however used a thermophilic instead of a mesophilic host for selection, allowed for the stabilisation of the activated monomer. Remarkably, none of the identified exchanges led to the re-dimerisation of sAnPRT, confirming the finding that an increased association state is only one of numerous mechanisms to stabilize a protein [2]. The analysis of the activated and the stabilized variants suggest that conformational flexibility of sAnPRT required for efficient catalysis goes at the cost of thermal stability. These findings underline the notion that protein engineering approaches can be highly instructive provided that the isolated variants are subjected to a detailed characterisation by protein chemistry, enzyme kinetics, and crystal structure analysis.

References

[1] Stetter, K.O. (2006) History of discovery of the first hyperthermophiles. *Extremophiles* **10:**357 – 362.
doi: http://dx.doi.org/10.1007/s00792-006-0012-7.

[2] Sterner, R. and Liebl, W. (2001) Thermophilic adaptation of proteins. *Crit. Rev. Biochem. Mol. Biol.* **36:**39 – 106.
doi: http://dx.doi.org/10.1080/20014091074174.

[3] Vieille, C. and Zeikus, G.J. (2001) Hyperthermophilic enzymes: Sources, uses, and molecular mechanisms for thermostability. *Microbiol. Mol. Biol. Rev.* **65:**1 – 43.
doi: http://dx.doi.org/10.1128/MMBR.65.1.1-43.2001.

[4] Jaenicke, R. and Böhm, G. (1998) The stability of proteins in extreme environments. *Curr. Opin. Struct. Biol.* **8:**738 – 748.
doi: http://dx.doi.org/10.1016/S0959-440X(98)80094-8.

[5] Benkovic, S.J. and Hammes-Schiffer, S. (2003) A perspective on enzyme catalysis. *Science* **301:**1196 – 1202.
doi: http://dx.doi.org/10.1126/science.1085515.

[6] Zavodszky, P., Kardos, J., Svingor, and Petsko, G.A. (1998) Adjustment of conformational flexibility is a key event in the thermal adaptation of proteins. *Proc. Natl. Acad. Sci. U.S.A.* **95:**7406 – 7411.
doi: http://dx.doi.org/10.1073/pnas.95.13.7406.

[7] Jaenicke, R. (1991) Protein stability and molecular adaptation to extreme conditions. *Eur. J. Biochem.* **202:**715 – 728.
doi: http://dx.doi.org/10.1111/j.1432-1033.1991.tb16426.x.

[8] Hernandez, G., Jenney, F.E., Jr., Adams, M.W., and LeMaster, D.M. (2000) Millisecond time scale conformational flexibility in a hyperthermophile protein at ambient temperature. *Proc. Natl. Acad. Sci. U.S.A.* **97:**3166 – 3170.
doi: http://dx.doi.org/10.1073/pnas.97.7.3166.

[9] Jaenicke, R. (2000) Do ultrastable proteins from hyperthermophiles have high or low conformational rigidity? *Proc. Natl. Acad. Sci. U.S.A.* **97:**2962 – 2964.
doi: http://dx.doi.org/10.1073/pnas.97.7.2962.

[10] Eijsink, V.G., Bjork, A., Gaseidnes, S., Sirevag, R., Synstad, B., van den Burg, B., and Vriend, G. (2004) Rational engineering of enzyme stability. *J. Biotechnol.* **113:**105 – 120.
doi: http://dx.doi.org/10.1016/j.jbiotec.2004.03.026.

[11] Bershtein, S. and Tawfik, D. S. (2008) Advances in laboratory evolution of enzymes. *Curr. Opin. Chem. Biol.* **12:**151 – 158.
doi: http://dx.doi.org/10.1016/j.cbpa.2008.01.027.

[12] Sterner, R. and Brunner, E. (2008) Relationships among catalytic activity, structural flexibility, and conformational stability as deduced from the analysis of mesophilic-thermophilic enzyme pairs and protein engineering studies, In *Thermophiles – Biology and technology at high temperatures* (Robb, F., Antranikian, G., Grogan, D., and Driessen, A., Eds.), pp 25 – 28, CRC press, Taylor & Francis Group, LLC, Boca Raton.

[13] Sinha, S.C. and Smith, J.L. (2001) The PRT protein family. *Curr. Opin. Struct. Biol.* **11:**733 – 739.
doi: http://dx.doi.org/10.1016/S0959-440X(01)00274-3.

[14] Marino, M., Deuss, M., Svergun, D.I., Konarev, P.V., Sterner, R., and Mayans, O. (2006) Structural and mutational analysis of substrate complexation by anthranilate phosphoribosyltransferase from *Sulfolobus solfataricus*. *J. Biol. Chem.* **281:**21410 – 21421.
doi: http://dx.doi.org/10.1074/jbc.M601403200.

[15] Ivens, A., Mayans, O., Szadkowski, H., Wilmanns, M., and Kirschner, K. (2001) Purification, characterization and crystallization of thermostable anthranilate phosphoribosyltransferase from *Sulfolobus solfataricus*. *Eur. J. Biochem.* **268:**2246 – 2252.
doi: http://dx.doi.org/10.1046/j.1432-1327.2001.02102.x.

[16] Schwab, T., Skegro, D., Mayans, O., and Sterner, R. (2008) A rationally designed monomeric variant of anthranilate phosphoribosyltransferase from *Sulfolobus solfataricus* is as active as the dimeric wild-type enzyme but less thermostable. *J. Mol. Biol.* **376:**506 – 516.
doi: http://dx.doi.org/10.1016/j.jmb.2007.11.078.

[17] Schlee, S., Deuss, M., Bruning, M., Ivens, A., Schwab, T., Hellmann, N., Mayans, O., and Sterner, R. (2009) Activation of anthranilate phosphoribosyltransferase from *Sulfolobus solfataricus* by removal of magnesium inhibition and acceleration of product release. *Biochemistry* **48:**5199 – 5209.
doi: http://dx.doi.org/10.1021/bi802335s.

[18] Wang, G.P., Lundegaard, C., Jensen, K.F., and Grubmeyer, C. (1999) Kinetic mechanism of OMP synthase: A slow physical step following group transfer limits catalytic rate. *Biochemistry* **38:**275 – 283.
doi: http://dx.doi.org/10.1021/bi9820560.

[19] Codreanu, S.G., Ladner, J.E., Xiao, G., Stourman, N.V., Hachey, D.L., Gilliland, G.L., and Armstrong, R.N. (2002) Local protein dynamics and catalysis: detection of segmental motion associated with rate-limiting product release by a glutathione transferase. *Biochemistry* **41:**15161 – 15172.
doi: http://dx.doi.org/10.1021/bi026776p.

[20] Schwab, T. and Sterner, R. (2011) Stabilization of a metabolic enzyme by library selection in *Thermus thermophilus*. *ChemBioChem* **12:**1581 – 1588.
doi: http://dx.doi.org/10.1002/cbic.201000770.

[21] Miles, E.W., Rhee, S. and Davies, D.R. (1999) The molecular basis of substrate channeling: *J. Biol. Chem.* **274:**12193 – 12196.
doi: http://dx.doi.org/10.1074/jbc.274.18.12193.

[22] Raushel, F.M., Thoden, J.B., and Holden, H.M. (2003) Enzymes with molecular tunnels: *AccChemRes* **36:**539 – 548.
doi: http://dx.doi.org/10.1021/ar020047k.

[23] Thoma, R., Hennig, M., Sterner, R., and Kirschner, K. (2000) Structure and function of mutationally generated monomers of dimeric phosphoribosylanthranilate isomerase from *Thermotoga maritima*. *Structure Fold. Des.* **8:**265 – 276.
doi: http://dx.doi.org/10.1016/S0969-2126(00)00106-4.